

Article

Performance of Regenerated Activated Carbons on Pesticides Removal from the Aqueous Phase

Isabel Pestana da Paixão Cansado ^{1,2,*} , Paulo Alexandre Mira Mourão ¹ 
and José Eduardo dos Santos Félix Castanheiro ¹ 

¹ MED—Mediterranean Institute for Agriculture, Environment and Development & Change—Global Change and Sustainability Institute, Departamento de Química e Bioquímica, Escola de Ciências e Tecnologia, Universidade de Évora, Rua Romão Ramalho n° 59, 7000-671 Évora, Portugal; pamm@uevora.pt (P.A.M.M.); jefc@uevora.pt (J.E.d.S.F.C.)

² LAQVRequimte, Universidade de Évora, Rua Romão Ramalho n° 59, 7000-671 Évora, Portugal

* Correspondence: ippc@uevora.pt

Abstract: Adsorbents presenting high adsorption capacity, fast adsorption rate, easy regeneration, and a good possibility for reusability are ideal for removing 4-chloro-2-methyl-phenoxyacetic acid (MCPA) or other pesticides from wastewater. Here, the effects of regeneration treatments on adsorption–desorption cycles are examined using two commercial activated carbons (ACs) (Merck and Norit 1240 X). MCPA adsorption was fast on Merck and Norit ACs in powder form (6 h) but on Norit AC, in granular form, adsorption was too slow, and the equilibrium time was reached only after 288 h. MCPA adsorption kinetic data were analyzed by applying pseudo-first-order, pseudo-second-order, and Weber–Morris models. The pseudo-second-order model fit better to all data, and the Weber–Morris representation allows confirming that on Norit 1240 X, in granular form, the pore diffusion was the limiting factor concerning the MCPA adsorption. Merck and Norit 1240 X (in powder and granular form) ACs loaded with MCPA were submitted to different regeneration process by washing with distilled water, ethanol, HNO₃, and NaOH solutions and washed with NaOH solutions or ethanol followed by a thermal treatment. The ACs regenerated with ethanol performed well in the subsequent adsorption–desorption cycles. All ACs had more than 99% desorbed MCPA after the first cycle of washing with ethanol. The washing with NaOH solution was less efficient. The regeneration process, consisting of washing the sample with a solution of NaOH and subsequent heating at 573 K, was very effective. After this regeneration procedure, the amount of MCPA adsorbed on Norit 1240 X AC was even higher than the amount adsorbed in the first adsorption cycle. At present, washing methods for adsorbent regeneration are not used at an industrial level. However, research for environmentally friendly regeneration methods is necessary to achieve the objectives of the circular economy.

Keywords: activated carbon regeneration; pesticide removal; reuse; circular economy



Citation: Cansado, I.P.d.P.; Mourão, P.A.M.; Castanheiro, J.E.d.S.F. Performance of Regenerated Activated Carbons on Pesticides Removal from the Aqueous Phase. *Processes* **2023**, *11*, 2496. <https://doi.org/10.3390/pr11082496>

Academic Editor: Avelino Núñez-Delgado

Received: 31 July 2023

Revised: 11 August 2023

Accepted: 17 August 2023

Published: 19 August 2023



Copyright: © 2023 by the authors. Licensee MDPI, Basel, Switzerland. This article is an open access article distributed under the terms and conditions of the Creative Commons Attribution (CC BY) license (<https://creativecommons.org/licenses/by/4.0/>).

1. Introduction

Pesticides are increasingly being discovered in wastewater and natural water bodies as a result of their excessive use in agro-industrial activities (agricultural and veterinary). It is challenging to establish a global approach that will enable the removal of pesticides from liquid effluents due to the large variety of pesticides (herbicides, fungicides, acaricides, etc.) that may be found on the market [1].

In reviews by Kulaishin et al. 2022 [2] and Baskar et al. 2022 [3], adsorption on a variety of adsorbents, particularly on activated carbon (ACs), was emphasized as one approach for removing pesticides from the aqueous phase. There are certain drawbacks to other methods now in use, including the time needed for the process and reliance on environmental conditions for the biodegradation process, the need for energy for electrooxidation, and the photocatalytic process [2].

Adsorption is an efficient technique for eliminating inorganic and organic pollutants from gaseous effluents [3,4], as well as from liquid effluents such as drinking water and sewage [3]. Adsorption is currently used, although it presents some limitations, such as adsorbent production cost, regeneration, and sustainable management of spent adsorbents [2–6].

Commercial ACs have traditionally been produced from expensive materials, including wood, coal, coconut shells, lignite, petroleum residues, and coal. The use of alternative precursors, such as agricultural and agro-industrial wastes, was studied in order to decrease the use of nonrenewable precursors and the cost of ACs.

ACs produced from a variety of precursors have been successful in removing pollutants from the liquid phase. Examples include the removal of pesticides (4-chloro-2-methylphenoxyacetic acid and diuron) with ACs prepared from *Tectona Grandis* [7–9], dyes with ACs prepared from different biomass, activated with KOH, NaOH, and H₂SO₄ [9,10], Cu²⁺, Zn²⁺, and Pb²⁺ with ACs prepared from *Phaseolus aureus* hulls, activated with steam [11], As³⁺ with granulated biochar [12], and pharmaceutical products with ACs prepared from waste materials and wood [13,14].

Adsorption in ACs is widely applied because of its efficiency, high adsorption capacity, and easy applicability on a large scale. Still, it presents some disadvantages. If treated incorrectly, the saturated adsorbents could result in secondary pollution. The adsorbates retained on the ACs' surfaces can be leached into the environment where the saturated adsorbents are dumped [3,4]. An effective management approach for saturated adsorbents must include regeneration and reuse. For the regeneration of spent adsorbents, thermal, chemical, and biological techniques are most frequently used [3,14–25]. In the industry, thermal regeneration entails sending a flow of steam or carbon dioxide over the saturated adsorbent at high temperatures (greater than 1000 K). This process promotes an increase in the porous volume by allowing for the desorption of contaminants, as well as the unlocking, enlargement, and formation of new pores. For heat regeneration to be effective in phenol desorption, there must be a significant energy demand and the presence of an oxidizing agent, which could result in an adsorbent burn-off of between 5 and 15% [22].

Chemical regeneration can be carried out by oxidizing chemical agents, washing the spent adsorbents with specific solvents, using acidic or basic solutions, or desorbing adsorbates [17]. How well these methods work depends on the interactions between the adsorbate and the used regeneration solvents and solutions and the interactions between the adsorbate and the adsorbent.

Bioregeneration is a simple and eco-friendly process that needs low investment to be implemented. However, adsorbates must be biodegradable to succeed, but this does not happen frequently, making the process time-consuming [3,20].

Recently, numerous studies have looked into the use of microwaves to shorten regeneration times and consume less energy [5]. A combination of microwave and ultraviolet irradiation was used to regenerate ACs saturated with chloramphenicol. Even after five adsorption/regeneration cycles, the adsorption efficacy of granular ACs was said to have been maintained at a high level, according to the authors [4]. Nevertheless, it was also recognized that the byproducts generated during the microwave regeneration process can be more harmful than the initial pollutants, particularly if the organic pollutants contain chlorine [5].

Additionally, a vacuum system was employed to assess the regeneration of saturated ACs by subjecting the saturated ACs to a vacuum source. A performance of 90% was allegedly maintained in ACs that had been saturated with toluene after five adsorption/desorption cycles [23]. With the exception of the thermal regeneration technique, these techniques are not currently being used in the industry [19,24,26].

When compared with the original one, regenerated ACs are less expensive. However, some characteristics lead to inferior performance when compared with the original ACs. The regenerated ACs may also retain some contaminants, which causes them to saturate more quickly in the long run [5].

In any case, there is a financial benefit to being able to use the same adsorbents repeatedly in the same process. On the other hand, the adsorbate can be employed to carry out its original role if it is successfully recovered.

The adsorption or desorption kinetics of MCPA will be investigated in this study, with a focus on the regeneration and reuse of spent ACs. Regeneration techniques included heat regeneration, washing regeneration, using different solutions and solvents, and a combination of washing and thermal regeneration.

2. Materials and Methods

On removal of MCPA from the aqueous phase, two commercial activated carbons were employed, both as received and after being submitted through various adsorption and regeneration process.

2.1. ACs Structural and Chemical Characterization

Both the ACs used, one from Merck (powder form), purchased from Sigma Aldrich, Madrid, Spain and the other from Norit (Norit 1240 X, in powder and granular form), purchased from Fisher Scientific, Lisbon, Portugal, were texturally and chemically characterized by nitrogen adsorption at 77 K, elemental analysis, and through the determination of the pH at the point of zero charge. The procedures used for these purposes are described elsewhere [8,26,27]. The surface of the ACs was also analyzed by ATR-FTIR spectroscopy analysis measurements, in the range between 450 and 4000 cm^{-1} , performed on a Perkin Elmer Spectrum Two IR spectrophotometer with an Attenuated Total Reflection (ATR) accessory, purchased from I.L.C., Lisbon, Portugal. A Phenom ProX Desktop Scanning Electron Microscope (SEM) instrument was used on the morphology characterization, with an accelerating voltage set to 5 to 15 kV, from I.L.C., Lisbon, Portugal.

2.2. Pesticide Adsorption from Liquid-Phase

4-Chloro-2-methylphenoxyacetic acid (MCPA), which was acquired from Sigma-Aldrich, Spain and had a stated purity of HPLC-Grade higher than 97.4%, was the adsorptive employed in the adsorption assays. The kinetics investigations were performed at 298 K, adding 10 mg of ACs to 25 mL of an aqueous solution containing 150 mg L^{-1} of MCPA at a pH of about 3. This was carried out in accordance with earlier research [28,29]. As the MCPA has a $\text{pK}_a = 3.73$, at 298 K [30], at a $\text{pH} < \text{pK}_a$, the MCPA is in neutral form, which increases the electrostatic attraction with the ACs surface, which is positively charged ($\text{pH}_{\text{pzc}} > 7.2$). At different time intervals, aliquots were removed from the solution and the amount of MCPA was determined. The MCPA adsorption isotherms were obtained from solutions whose concentrations vary from zero to 500 mg L^{-1} . The suspensions were left under an agitation of 20 rpm in a shaking bath, a Linear model—GRANT, purchased from VWR, Carnaxide, Portugal—at 298 K. After an adequate contact time, the residual concentration of the pesticide on the solution was assessed by UV/visible spectrophotometry using a Nicolet Evolution 300 UV-Vis Spectrophotometer, from Thermo Electron Corporation, purchased from Fisher Scientific, Portugal.

MCPA quantification was conducted through the absorbance values obtained at the wavelengths of 228 and 280 nm. By using an external pattern, such as a standard curve created for this purpose, the residual pesticide in the solution was quantified. The difference between the pesticide's initial concentration and its remaining concentration in solution, divided by the mass of the AC utilized and considering the volume of solution used, was used to calculate the amount of pesticide adsorbed ($Q_{\text{ads}}/\text{mg g}^{-1}$) on the ACs.

2.3. ACs Regeneration

To perform regeneration studies, the ACs were first saturated with MCPA. For that purpose, a fixed quantity of ACs (100 mg) was added to 100 mL of an aqueous solution containing 250 mg L^{-1} of MCPA. The AC's maximum adsorption capacity was assessed once the adsorption equilibrium was established. These assays were performed multiple

times, allowing the calculation of standard deviation and error. The supernatant was then removed, and different desorption experiments were performed. For this purpose, five different treatments were applied: (1) acid aqueous washing with HNO_3 (1 mol dm^{-3}); (2) basic aqueous washing with NaOH (0.01, 0.1, and 1.0 mol dm^{-3}); (3) washing with distillate water; (4) washing with ethanol; and a (5) two-step treatment, washing with aqueous solutions and ethanol and heating at 573 K for 30 min. The chemical characteristics of the spent and the regenerated ACs were obtained, and their performance was connected with those properties.

2.3.1. ACs Regeneration by Washing with Solvents

The saturated ACs were dried in an oven at 378 K until the mass remained constant. Once dried, the spent ACs were placed in a volume of 100 mL of ethanol or 100 mL of each of the tested washing solutions. The solutions used were the nitric acid solution, (1 mol dm^{-3} (pH around 1), ethanol, distilled water (pH = 6), and sodium hydroxide solutions, (0.001, 0.1 and 1 mol dm^{-3}). The suspensions were then put in a thermostable bath under the agitation of 70 rpm for 24 h. The supernatant was removed, and the desorption washing was repeated three times. After each cycle, the concentration of the pesticide in the supernatant was quantified, and the total amount of pesticide desorbed was calculated. The regenerated ACs were reused in a new adsorption cycle, and their performance in the removal of MCPA from the aqueous phase was evaluated.

2.3.2. AC Regeneration by Basic Aqueous Washing Followed by Thermal Treatment

The spent ACs, after three adsorption–desorption cycles, as described in Section 2.3.1, were recovered after the supernatant removal. Then, about 100 mg of the ACs, washed with different solvents, were placed in a steel container and put into a furnace, (High Temp Technology, TR–334/2018, from Thermolab). ACs were then submitted to a rate of 10 K min^{-1} until 573 K under a nitrogen flow rate of $85 \text{ cm}^3 \text{ min}^{-1}$ and kept for 30 min. The carbonaceous material was cooled down, always under the same nitrogen flow. The regenerated ACs were reused, and their performance was evaluated on MCPA removal from the aqueous phase.

3. Results and Discussion

3.1. Characterization of the Adsorbent Materials

Both ACs, Merck and Norit, were chemically characterized using the determination of the point of zero charge and elemental analysis, and their textural characteristics were based on N_2 adsorption at 77 K [28]. The findings are shown in Table 1 to help with the discussion of the results.

Table 1. Chemical and textural characteristics of the Merck and Norit 1240 X ACs. In Table 1, A_{BET} is the apparent surface area, obtained using the BET method, V_s is the total porous volume, A_s is the external surface area (V_s and A_s were obtained using the alfa-s method), V_0 is the volume of the micropores, and L_0 is the mean pore size (V_0 and L_0 were obtained using the Dubinin–Radushkevich method).

Activated Carbon	$A_{\text{BET}}/\text{m}^2 \text{ g}^{-1}$	$A_s/\text{m}^2 \text{ g}^{-1}$	$V_s/\text{cm}^3 \text{ g}^{-1}$	$V_0/\text{cm}^3 \text{ g}^{-1}$	L_0/nm	C/%	H/%	S/%	pHpzc
Norit 1240 X	975	60	0.43	0.23	1.04	84.4	0.19	0.49	9.73
Merck	927	170	0.36	0.23	1.02	85.2	0.22	0.32	7.27

Norit 1240 X was characterized through nitrogen adsorption in granular form. As seen in Table 1, it presents a slightly high apparent surface area and total porous volume, with a similar micropore volume and means pore size when compared with the AC from Merck. These results suggest that the efficacy of the ACs against MCPA adsorption will not be considerably impacted by textural characteristics. Comparing Norit 1240 X with Merck AC, which has a more basic nature (pHpzc = 9.73 vs. 7.27) (Table 1), suggests that this difference

may have some bearing on how contaminants are removed from the aqueous phase. The surface of the ACs was examined using ATR-FTIR spectroscopic analysis and SEM-EDX after they were received, saturated with MCPA, and regenerated using various processes.

3.2. Chemical Characterization of the Adsorbent Materials

To verify the influence of the MCPA adsorption and regenerations treatments on the ACs' surface, they were characterized by SEM-EDX and FTIR. Figure 1a,b illustrates the surface morphology of ACs before MCPA adsorption, Figure 1c illustrates the ACs' surface covered by an MCPA white film, and Figure 1d shows the ACs' surface after being saturated and regenerated by washing method followed by a thermal treatment.

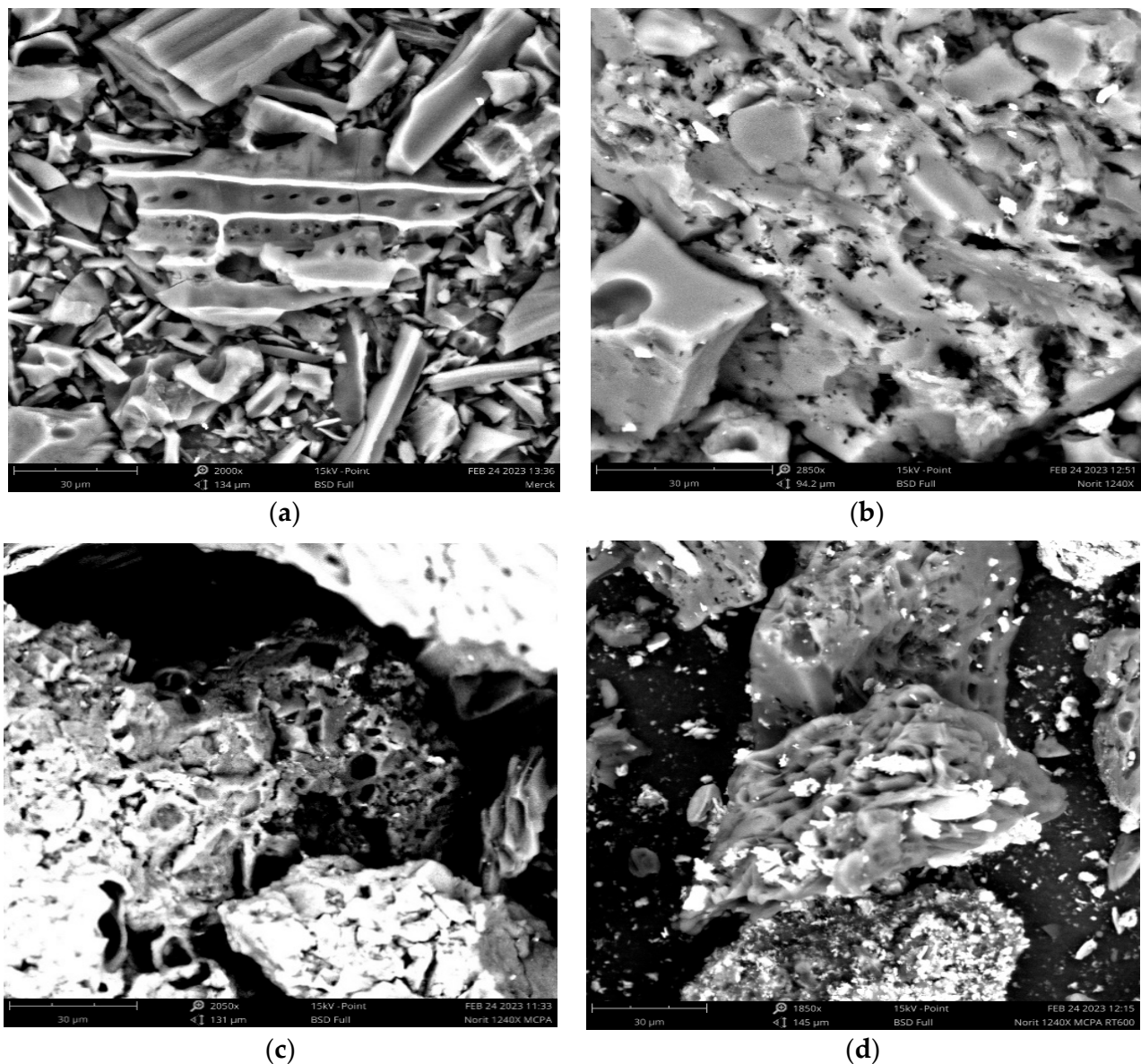


Figure 1. SEM images were obtained at different stages of the MCPA adsorption–desorption cycle. (Norit 1240 X_p + MCPA–RT means saturated MCPA–AC after being regenerated by washing with NaOH (0.01 mol dm^{−3}) and thermal temperature at 573 K): (a) Merck original AC; (b) Norit 1240 X_p original AC; (c) Norit 1240 X_p + MCPA; (d) Norit 1240 X_p + MCPA–RT.

In Figure 1c, an MCPA film covers the ACs surfaces and hinders their adsorption activity due to the blockage of the pores, even though it is possible to see that the cavities

were not completely blocked. The thermal treatment allows the desorption of MCPA from the ACs' surfaces, as shown in Figure 1d.

FTIR spectroscopy was used to learn more about the surface functional groups at various stages of the adsorption–desorption cycle (as illustrated in Figure 2). The spectra presented are from Norit AC. In Figure 2, the broader band from 3020 to 3300 cm^{-1} was related to the O-H group. The interferences of the O-H group were identified around 1420 cm^{-1} and at 880 cm^{-1} , which reflected the contribution of O-H in deformation mode. These two bands were less expressed on the ACs regenerated with a NaOH solution followed by thermal regeneration (Norit 1240 X-RT). The decrease in the intensity of the bands can be attributed to the decomposition of the functional groups containing oxygen at high temperatures, as reported by Liao et al. [26].

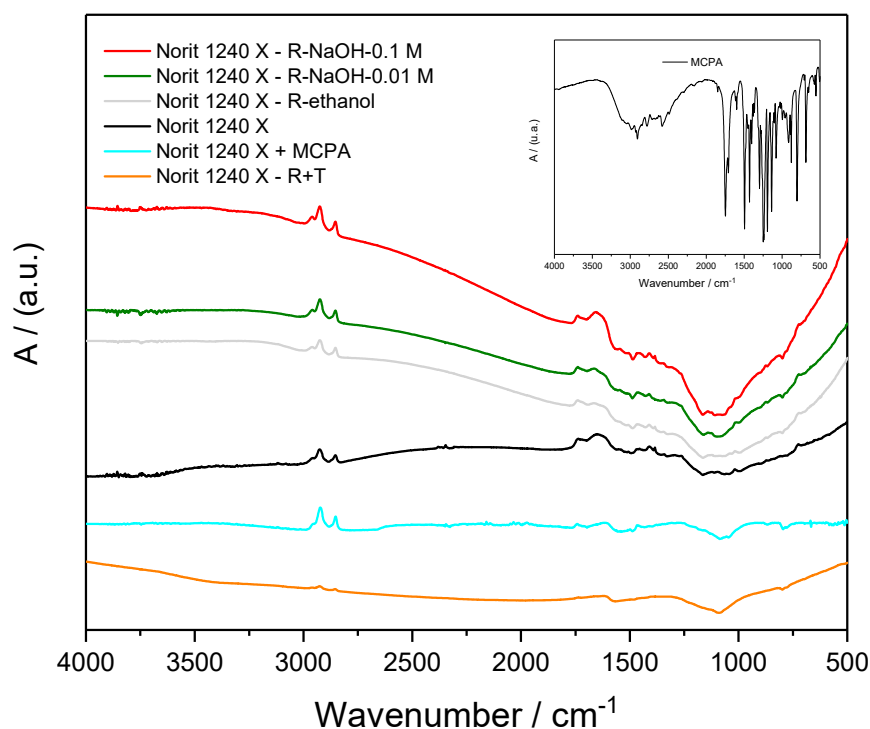


Figure 2. FTIR spectra were obtained on the Norit 1240 X AC at different steps in the MCPA adsorption–desorption cycles.

The bands at 2945 and 2889 cm^{-1} are characteristics of the alkyl groups, namely CH_3 and CH_2 . The band at 790 cm^{-1} allows the identification of the C-H groups on the alkenes' structures on a benzene structure. The bands at 1560 and 1680 cm^{-1} could be due to the C=C in a cyclic structure. The band at 1760 cm^{-1} could be attributed to the C=O bond on a carboxylic or ester group. Both bands were less present on the ACs regenerated with NaOH solution followed by a thermal treatment. The bands present at 1089 and 1200 cm^{-1} could be due to the C-O bond on primary and secondary alcohol, respectively.

With regard to the identification of possible changes in the profiles of the FTIR spectra due to the presence of MCPA, it is possible to deduce its presence simply by comparing the spectra of the various samples with the spectrum of MCPA (top right). It is of note that its characteristic bands and peaks (specifically in the region 3250–2500 cm^{-1} , 1750–750 cm^{-1}) intensify the bands and peaks already identified in the Norit X_p + MCPA samples. In the spectra of Norit 1240 X + MCPA, a small band around 780 cm^{-1} is more pronounced than in the other spectra. However, the bands regarding MCPA are present in the spectra of Norit 1240 X + MCPA, but they are masked by the bands of the AC. In the case of the samples regenerated with NaOH and ethanol, their influence seems to be less as one moves from regeneration with the basis solution to with alcohol. On the other hand,

the samples regenerated by the thermal process show a much lower MCPA contamination, reflecting the efficiency of this process.

3.3. MCPA Kinetic Studies

The adsorption capacity of ACs for different pollutants, in the aqueous phase, depends on numerous factors, and this complexity represents a challenge for researchers. Prior optimizations were made to some of the factors affecting the removal of MCPA by ACs from the aqueous phase [7]. Based on these conditions, the MCPA adsorption was carried out from a solution in which the pH was adjusted to 3. The time needed to establish the adsorption equilibrium was evaluated on Merck (powder form) and Norit 1240 in granular (Norit 1240 X_g) and powder form (Norit 1240 X_p) from a solution containing 150 mg L⁻¹ of MCPA, and the results are shown in Figure 3.

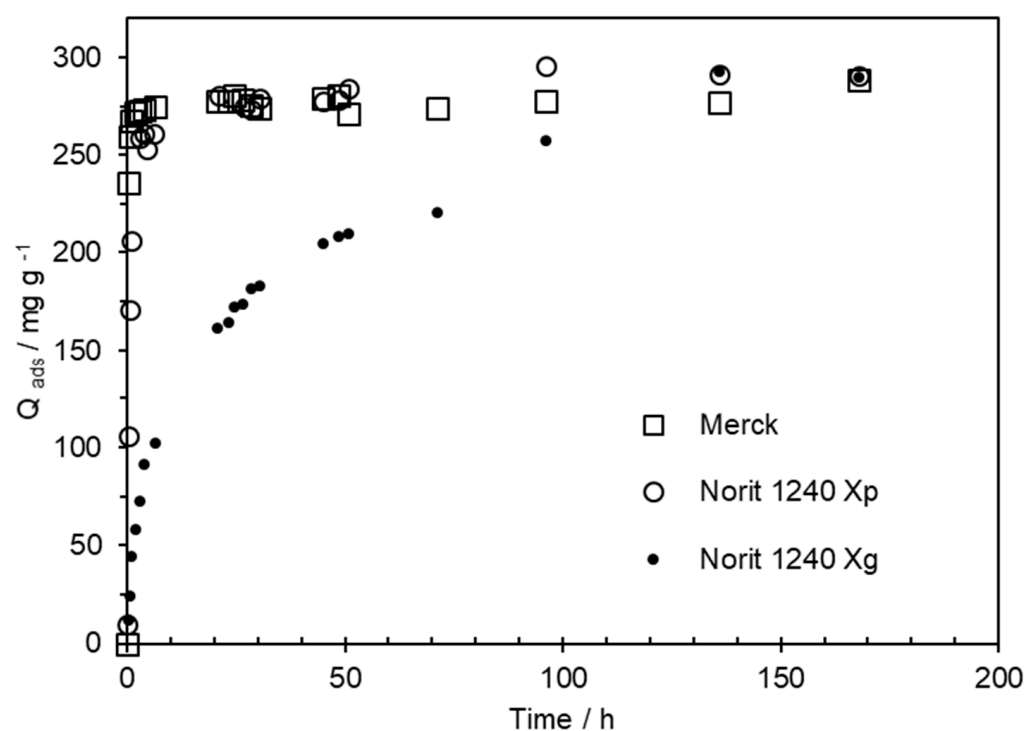


Figure 3. Kinetic study of MCPA adsorption in Norit 1240 X (in granular form—Norit 1240 X_g—and powder form—Norit 1240 X_p) and Merck ACs in powder form. The kinetic studies were conducted with a solution containing 150 mg L⁻¹ of MCPA.

On Merck and Norit 1240 X_p (powder form) ACs, the equilibrium of the MCPA adsorption process was achieved after a contact time of 6 h. But, with Norit 1240 X_g, the maximum adsorption capacity was reached only after a long contact time (288 h). In practical terms, a contact period of more than 24 h is unrealistically long, especially in spill situations where the AC must have a high adsorption capacity. But most importantly, the adsorption must be fast. To avoid the problems related to obtaining data, when the equilibrium has not yet been completely achieved, the isotherms were subsequently obtained at different time intervals of up to 288 h.

The experimental data obtained during the kinetic study were fitted by the pseudo-first-order (PFO) and pseudo-second-order (PSO) kinetic models to assess the mechanisms of the adsorption kinetics. Equation (1) represents how the pseudo-first-order model might be expressed.

$$\ln(Q_{\max} - Q_{\text{ads}}) = \ln(Q_{\max}) - K_1 \times t \quad (1)$$

The data from the pseudo-first-order model are obtained by plotting $\ln(Q_{\max} - Q_{\text{ads}})$ vs. t .

The pseudo-second-order model can be expressed by Equation (2).

$$T/Q_{\text{ads}} = 1/(K_2 \times (Q_{\text{max}})^2) + 1/Q_{\text{max}} \times t \quad (2)$$

The data from the pseudo-second-order are obtained by plotting (t/Q_{ads}) vs. t [31]. The slope of Equation (2) was related to the initial rate of the adsorption using the following expression: $1/(K_2 \times (Q_{\text{max}})^2) = 1/V_0$.

In Equations (1) and (2), Q_{max} and Q_{ads} are the MCPA amounts adsorbed after a contact time of 288 h and at a time t (mg g^{-1}); K_1 is the equilibrium rate constant of pseudo-first-order reaction (h^{-1}); K_2 is the equilibrium rate constant of pseudo-second-order reaction (h^{-1}); and V_0 is the initial adsorption rate. The PFO model is less applicable when the time needed to reach equilibrium is too long or simply not reached. To avoid this limitation, mainly concerning the adsorption in Norit 1240 X_g , in the three systems, the Q_{max} was obtained after a contact time of 288 h. On Merck and Norit 1240 X_p , this value is quite similar to that obtained after a contact time of 24 h.

The data obtained with both equations are included in Table 2. The R^2 values presented in Table 2 show that the pseudo-second-order model fits well with the experimental data when compared with the pseudo-first-order one, in agreement with Tochetto et al. 2023 [32] and data presented by Revellame et al. 2020 [33]. The values of the maximum amount of MCPA calculated by the pseudo-second-order model ($Q_{\text{max, cal2}}$) are quite similar to the values obtained experimentally ($Q_{\text{max, exp}}$), except for the Norit 1240 X_g .

Table 2. Parameters of the application of pseudo-first-order and pseudo-second-order models. The kinetic studies were conducted with a solution with 250 mg L^{-1} of MCPA.

ACs	$Q_{\text{max, exp}} / \text{mg g}^{-1}$	Pseudo-First-Order Model			Pseudo-Second-Order Model			
		$Q_{\text{max1, cal1}} / \text{mg g}^{-1}$	K_1 / h^{-1}	R^2	$Q_{\text{max, cal2}} / \text{mg g}^{-1}$	$V_0 / \text{mg g}^{-1} \text{ h}^{-1}$	K_2 / h^{-1}	R^2
Merck	288.1	10.2	0.0086	0.95	277.8	5000	0.13	0.98
Norit 1240 X_p	290.7	3.1	0.019	0.75	285.7	833	0.020	0.99
Norit 1240 X_g	289.6	10.3	0.011	0.99	188.7	52.6	0.0015	0.96

Simonin, in 2016, stated that an R^2 higher than 0.8 indicates a good fit between the data [31]. The adjustment of the PFO model to Norit 1240 X_p gives an R^2 of 0.75; hence, it is clear that the PFO adjustment was not adequate. With Norit 1240 X_g and Merck, the PFO adjustment presents an R^2 higher than 0.95. However, the maximum amounts adsorbed obtained from the PFO adjustment are quite far from the experimental value.

The adjustment to the PSO model presented an R^2 higher than 0.96 for the three systems. The Norit 1240 X_g presented a high R^2 , but the maximum amount of MCPA adsorbed obtained from the PSO model was only 65% of the amount obtained experimentally. Yet, our results are in the same direction as the conclusions arrived at by Revellame et al. 2020. In a review conducted in 2020, these authors concluded that the PSO kinetics provided the best correlation of experimental data on a diversity of analyzed published works [33].

The removal of pollutants from the aqueous phase can be controlled by the external transport from the liquid phase to the solid external surface by the access of the pollutants to the solid pores and by diffusion into the micropore. The data were plotted based on the Weber–Morris equation to better understand the limiting step in the MCPA adsorption processes, as presented in Figure 4 and Table 3. The Weber–Morris model is expressed by Equation (3). K_{ip} is the intraparticle diffusion rate constant ($\text{mg g}^{-1} \text{ h}^{1/2}$), and C is a constant related to the thickness of the adsorption boundary layer [26,30–33].

$$Q_{\text{ads}} = K_{\text{ip}} \times t^{1/2} + C \quad (3)$$

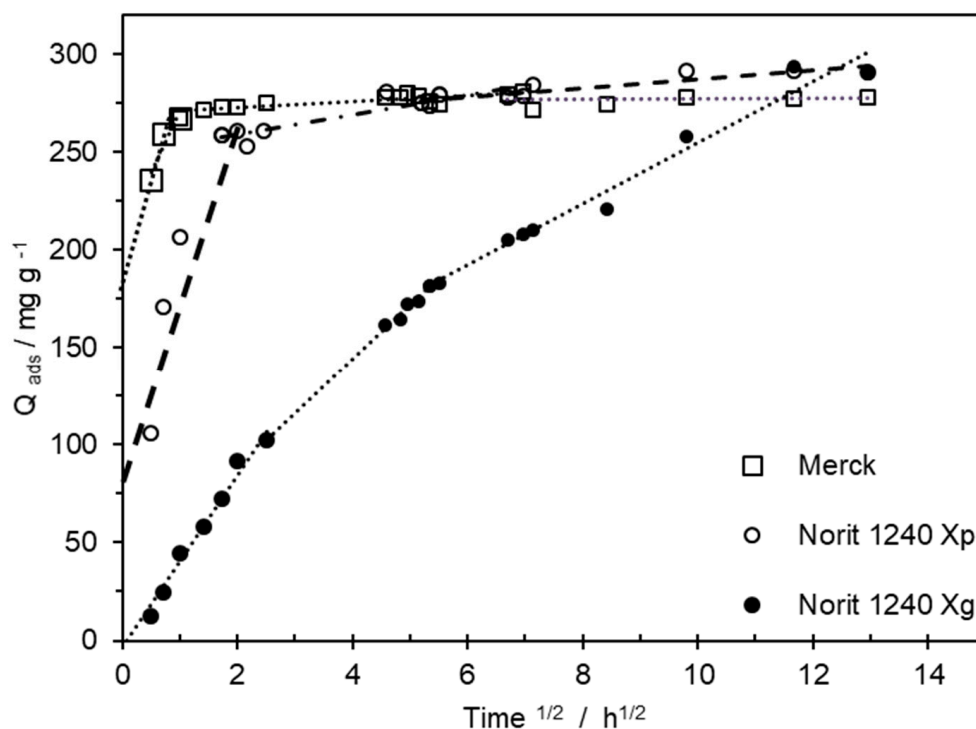


Figure 4. Weber–Morris or intraparticle diffusion plot for the experimental kinetic data.

Table 3. Parameters from the application of the Weber–Morris model. The kinetic studies were conducted with a solution containing 250 mg L^{-1} of MCPA. K_{ip1} , K_{ip2} , and K_{ip3} are intraparticle diffusion rate constants for the first, second, and third adsorption steps, respectively.

ACs	$Q_{ads} \text{ (max)}$ mg g^{-1}	K_{ip1} $\text{mg g}^{-1} \text{ h}^{1/2}$	C	K_{ip2} $\text{mg g}^{-1} \text{ h}^{1/2}$	C	K_{ip3} $\text{mg g}^{-1} \text{ h}^{1/2}$	C
Merck	288.1	114.0	178.8	0.8	271.3	0.2	75.2
Norit 1240 X _p	290.7	112.2	74.8	4.7	249.8	3.2	264.0
Norit 1240 X _g	289.6	44.0	--	27.8	32.4	15.6	98.6

For the Merck and Norit 1240 X_p ACs, the representation of Q_{ads} versus $t^{1/2}$ presents three linear steps, but the second and third steps have a very similar slope. With both ACs, all linear regression intercepts the y-axis in a positive value. Based on the work by Liao et. al (2013), this allows stating that intraparticle diffusion is not the only rate-controlling step for MCPA adsorption [26]. The first step was attributed to the occupation of the available surface sites on the external surface area through electrostatic attraction. This adsorption step is responsible for the fast process of the pseudo-second-order model and for the high K_{ip1} values presented in Table 3. The Merck and Norit 1240 X_p ACs presented very high initial constant rates, which agrees with the kinetic profile presented in Figure 1.

The values of the intraparticle rate diffusion in the second and third steps are very small when compared with those obtained in the first step [34]. At this point, the superficial sites and porous volume available for the MCPA adsorption are now residual, and the adsorption rate is very low.

When the Weber–Morris representation is applied to the Norit 1240 X_g MCPA adsorption system, three well-defined linear regions appeared. The interception of the first linear regression with the Y-axis is close to zero (being even negative), which may indicate that the limiting factors in the adsorption process are mainly related to intraparticle diffusion. The values of K_{ip} decreased as the contact time increased in the three MCPA–ACs systems. However, the K_{ip1} obtained in Norit 1240 X_g is lower than the values obtained in the

other two ACs systems. Some essays were carried out increasing the speed of agitation to promote the contact between Norit 240 X_g and the MCPA present in the solution. However, doubling the agitation speed between tests, no significant changes were observed in the amounts of MCPA adsorbed for different contact times. These results allow confirming that on Norit 1240 X_g, during the first step, the vacant adsorption sites on the external surface are occupied; after that, the intraparticle rate diffusion is the main factor, or the limiting step, that controls the MCPA adsorption inside the narrow pores. These findings demonstrated that the adsorption process comprised both film diffusion and intraparticle diffusion.

3.4. Pesticide Removal from the Aqueous Phase

Adsorption isotherms were performed using MCPA solutions with concentrations varying from 5 to 500 mg L⁻¹, at a pH = 3, after different contact times (from 24 to 288 h), as presented in Figures 5 and 6. The maximum adsorption capacity attains 401.3 mg g⁻¹ on Norit 1240 X_p, 392.2 mg g⁻¹ on Merck, and 403.7 mg g⁻¹ on Norit 1240 X_g after a contact time of 288 h, as shown in Figures 5 and 6. Some assays were conducted in triplicate (or even more) and were very reproducible, with a maximum standard deviation of 5 mg g⁻¹.

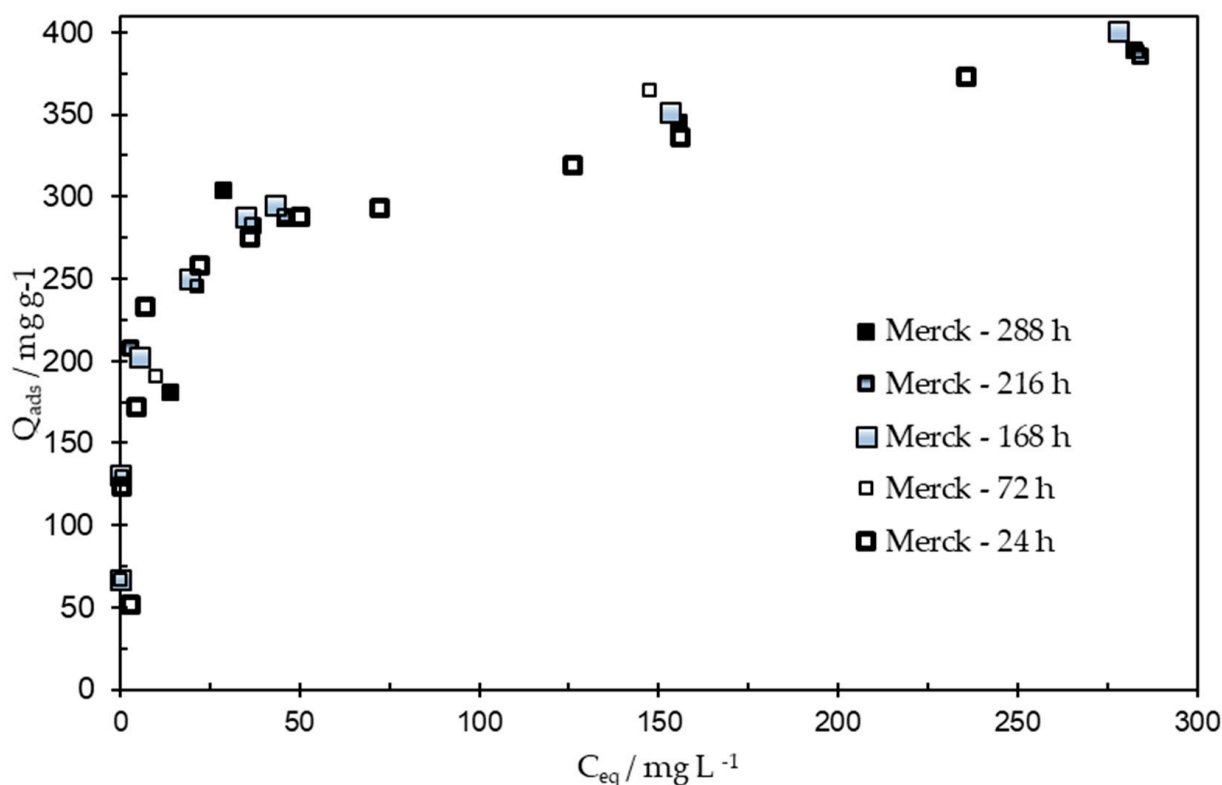


Figure 5. MCPA adsorption isotherms obtained on the ACs from Merck after different contact times.

After a contact time of 288 h, the amount of MCPA adsorbed on Norit AC in powder or granular form was similar. The longer contact times needed to achieve the adsorption equilibrium could explain the scattering of data points (data not presented here), mainly for shorter contact time. These results corroborate those obtained during the kinetic studies and allow us to rule out the diffusion of MCPA in the solution as a limiting factor.

Previous studies have led to the conclusion that the effect of the entry of adsorbate into the pores occurs only when the average pore diameter is less than 1.5 to 1.7 times the second widest dimension of the adsorbate [27,28]. The Norit 1240 X_g AC presents a mean pore size of 1.04 nm, and MCPA presents a molecular diameter between 7 and 9 Å [27].

This comparison allows confirming that the pore size exclusion effects seem not to be the predominant factor in the MCPA–Norit 1240 X_g system.

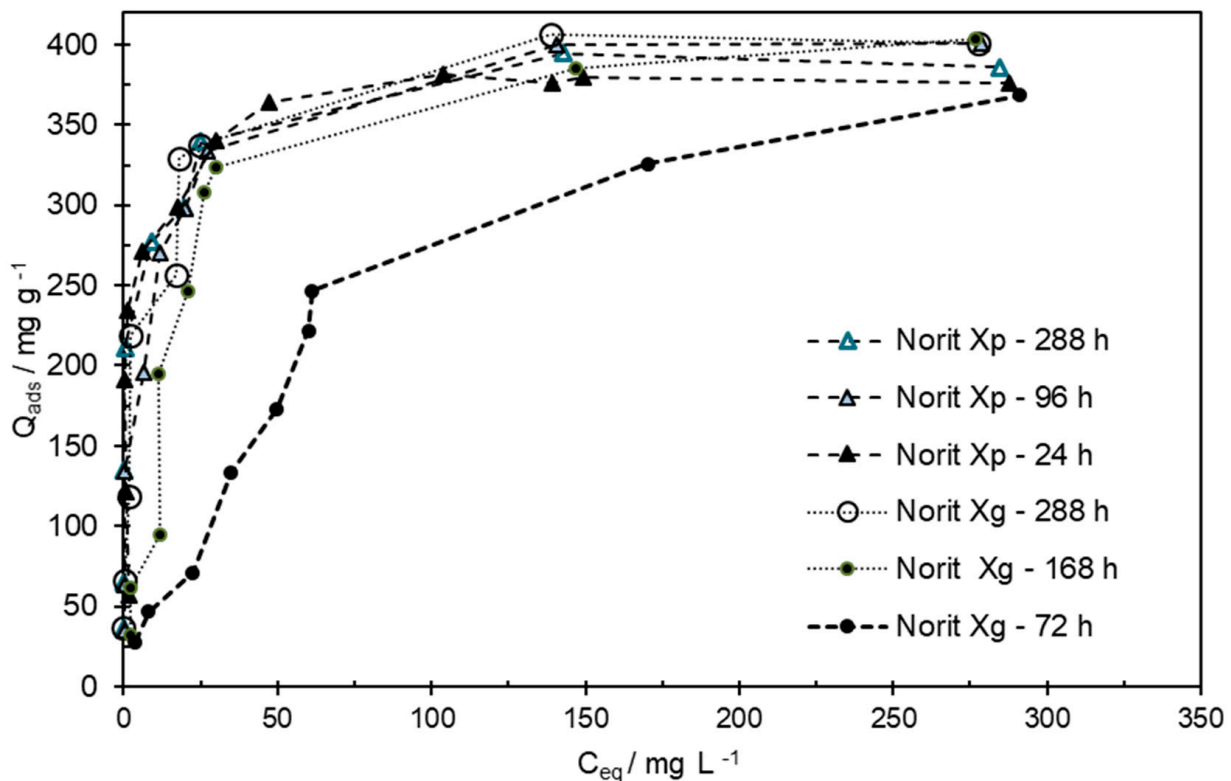


Figure 6. MCPA adsorption isotherms obtained on Norit 1240 X_p and Norit 1240 X_g after different contact times (between 24 and 288 h).

It is interesting to note that after a contact time of 288 h, the amount of MCPA adsorbed for higher concentrations is almost similar to that obtained by Norit 1240 X_p, shown in Figure 6. This finding allows us to confirm that on Norit 1240 X_g, the pore volume is available to the pesticide, and the diffusion in the narrow pores or narrow pores' entrance could be a limiting factor for the slow adsorption rate of MCPA molecules.

The maximum amount of MCPA adsorbed by both ACs is in the range of values obtained by Spaltro et al. (2018). These authors reported an amount of MCPA adsorbed on commercial GAB AC and CPB obtained from the Langmuir equation as 599.8 and 399.9 mg g⁻¹, respectively. From the application of the Freundlich equation, the amounts of MCPA obtained were 10.42 and 125.7 mg g⁻¹ on a commercial GAB AC and CPB, respectively [29].

3.5. Regeneration of ACs

Because the adsorbent loses its efficiency after becoming saturated, the regeneration process, or desorption of pollutants from the adsorbent, is crucial. Recent publications have emphasized the value of recycling used adsorbents rather than disposing of them [26,31,33]. The goal of the regeneration steps is to eliminate contaminants from the pores and external surface area without reducing the adsorption capacity. In this work, after being saturated with MCPA, the ACs were regenerated with different washing solutions and through thermal treatment. First, the same volume of six different solvents or solutions (ethanol, distilled water, NaOH—1, 0.1, and 0.01 mol dm⁻³, and HNO₃—0.1 mol dm⁻³) was added to a similar amount of saturated MCPA–ACs. These suspensions were kept in a thermostated bath under agitation at 298 K for 24 h.

The MCPA, which was previously retained in the ACs, thus moved into the solution [33]. According to the findings in Figure 7, which show the amount of MCPA desorbed from each AC, acidic solutions and distilled water are both inappropriate for the regeneration of MCPA-saturated ACs. These results are not surprising, since the adsorption of MCPA on different ACs was favored when performed from acidic solutions. In a review paper, Omorogie et. al (2016) reported that NaOH solutions were successfully used to desorb tannin and phenol from organoclays adsorbents. The same authors reported that HNO₃ solutions were useful to desorb MB from a composite adsorbent, and methanol was employed to regenerate carbonaceous adsorbents [14].

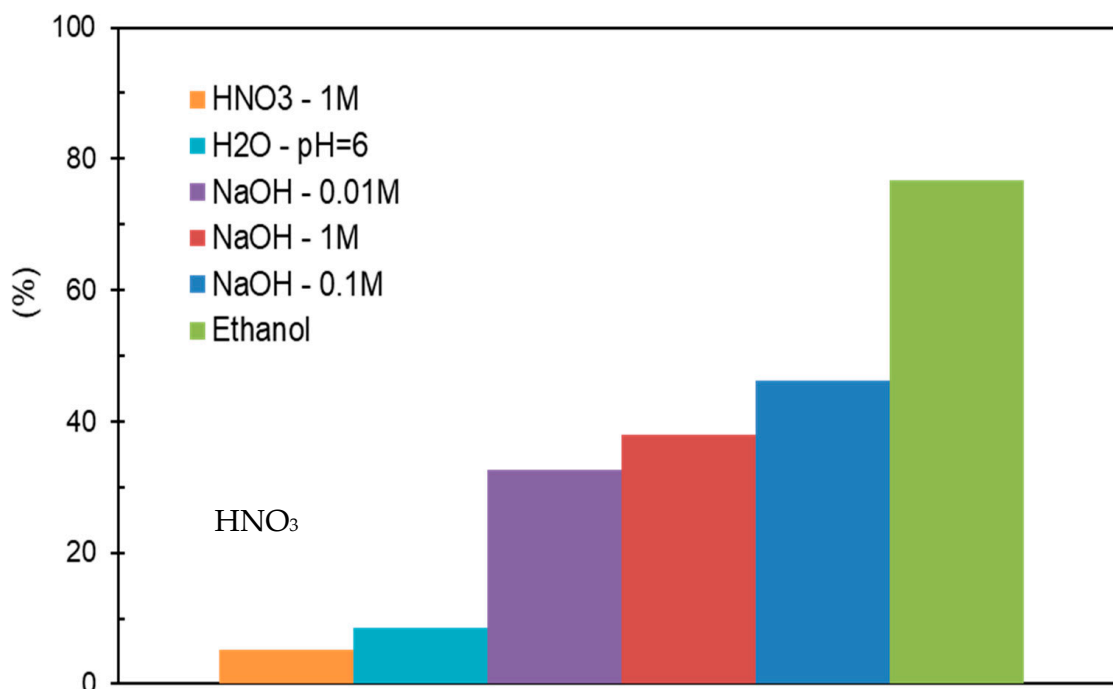


Figure 7. Percentage of MCPA desorbed from Merck AC using different washing solutions.

By using a single washing step, basic solutions and ethanol worked well on the regeneration of ACs. The follow-up of the different assays allowed us to verify that the desorption of the MCPA increases with the contact time between ACs and washing solutions. To promote the MCPA desorption on each regeneration cycle, mainly with ethanol or basic solutions, the saturated ACs were washed with 3×100 mL of ethanol or NaOH solutions (0.1 and 0.01 mol dm⁻³). The amount of MCPA that passed into the solution was quantified, and the regenerated ACs were used for a new adsorption cycle, as the data included in Table 4 and Figure 8 show.

On the Merck AC, on the first regeneration cycle, after a contact time of 24 h and using 100 mL of washing solution, the desorption percentage of MCPA achieved 37.7 and 43.7%, with NaOH of 0.1 and 0.01 mol dm⁻³, respectively. Ethanol washing allowed to reach a removal percentage of 69.2%, as shown in Figure 8. After 72 h, (3×100 mL washing steps), the desorption percentage of MCPA with the basic solutions reached 63.8 and 69.0%, with NaOH 0.1 and 0.01 mol dm⁻³, respectively. Yet, ethanol was allowed to reach a desorption percentage higher than 99%.

However, the amount of MCPA that passed through the solution was greater than the amount that was subsequently adsorbed. This statement allows inferring that spent Merck AC is deactivated due to various types of physicochemical interactions with the washing solutions. This might obstruct the highly developed porous structure, destroying or reducing the ability to remove MCPA molecules in the long run.

Table 4. Performance of ACs after different regeneration cycles in MCPA removal from the aqueous phase. R1, R2, and R3 mean the first, second, and third regeneration cycles (*—the adsorption cycle was extended up to 96 h).

Activated Carbon	Regeneration Cycles	Qads/ mg g ⁻¹	Qads/ mg g ⁻¹	Qads/ mg g ⁻¹
		NaOH— 0.1 mol dm ⁻³	NaOH— 0.01 mol dm ⁻³	Etanol
Merck	R1	229.7	230.7	231.6
	R2	169.9	176.4	197.3
	R3	76.3	55.7	96.5
	R4 – (R3 + T = 573 K)	124.6	147.4	182.7
Norit 1240 X _p (powder)	R1	226.9	232.2	231.9
	R2	207.4	178.0	212.1
	R3	79.2	67.4	88.8
	R4 – (R3 + T = 573 K)	230.4	221.9	239.4
Norit 1240 X _g (granules)	R1	157.9	148.6	155.8
	R2	84.5	103.3	102.8
	R2 + 96 h *	141.3	167.8	180.4
	R3	77.5	74.3	142.7
	R4 (R3 + T = 573 K)	126.1	154.3	181.8

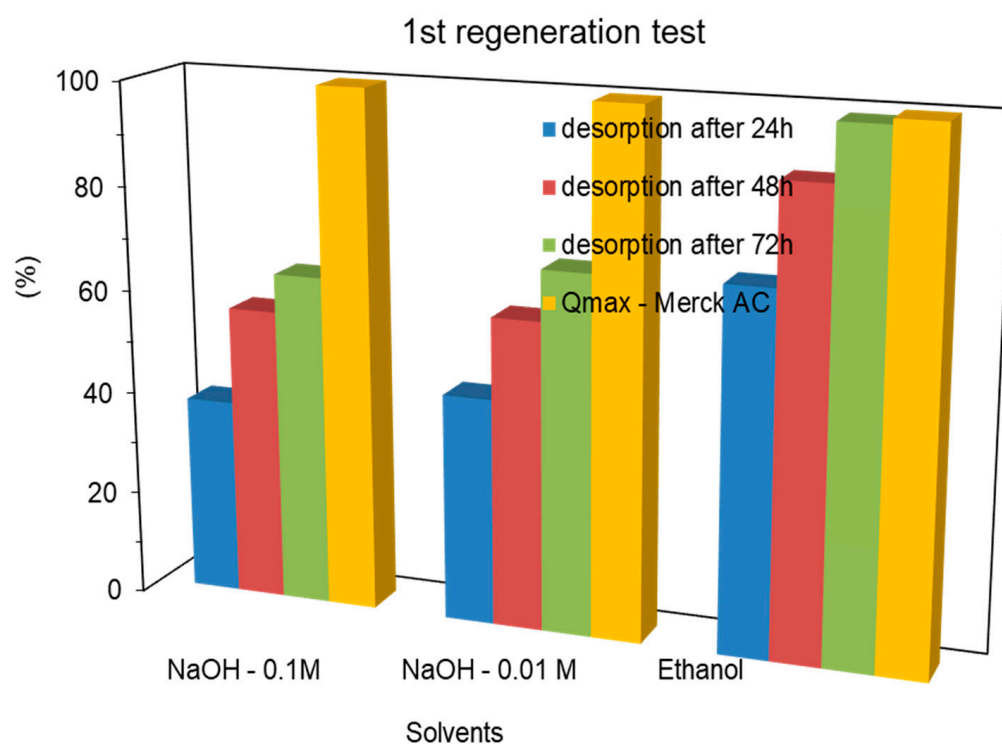


Figure 8. Percentage of MCPA desorption in the first regeneration process on Merck AC through washing methods using 100 mL of the washing solution every 24 h.

The second and third regeneration cycles of Merck AC led to a significant degradation of the adsorbent, which resulted in a successive decrease in the MCPA amount adsorbed in the different cycles (R1 to R3, Table 4). However, when the contact time between the adsorbent and MCPA was prolonged to 96 h, the amount of MCPA adsorbed increased. This finding leads to the conclusion that the different stages of washing the AC promote a reduction in pore intake, which makes it more difficult for MCPA to access pores, which may indicate that the limiting factors are mainly related to intraparticle diffusion.

Concerning Norit 1240 X_p in each adsorption cycle, the MCPA amount desorbed was lower than the amount desorbed on Merck, (54.2, 64.5, and 98.9% on ACs regenerated with NaOH 0.1 and 0.01 mol dm⁻³ and ethanol, respectively). Surprisingly, the amount of MCPA adsorbed on the regenerated ACs was similar to or even higher than the amount adsorbed on the Merck AC.

On Norit 1240 X_g, the amount of MCPA adsorbed showed greater deviations between the various assays. The washing procedure used on Norit 1240 X_g was less effective. And the amount of MCPA that passed through the solution on the first regeneration cycle was lower (30.3, 45.2, and 84.8% on ACs regenerated with NaOH 0.1 and 0.01 mol dm⁻³ and ethanol, respectively) when compared with that obtained from Merck or Norit 1240 X_p. After being submitted to one regeneration cycle, Norit 1240 X_g was reused on a new adsorption cycle of MCPA from the aqueous phase. The MCPA amount adsorbed on the second and third cycles was lower than the amount adsorbed in the previous adsorption cycle. Here, again, when the contact time was increased to 96 h, the amount of MCPA adsorbed increased, in agreement with data obtained during the obtention of the initial isotherms, as shown in Table 3 (R3*).

In Norit 1240 X_g AC, the maximum amount of MCPA adsorbed varied between 59 and 69% of the amount adsorbed in the same AC in powder form. In granular form, all porous volume is accessible to the nitrogen molecule, which is a small molecule. However, the restrictions in pore entrance limit access to large molecules, such as MCPA. This restriction in pore access explains the lower performance and slower kinetics presented by Norit X_g, as presented in Figures 4 and 6. Although the adsorption–desorption cycles obtained after prolonged contact times performed better, in practical settings, such as those involving spills, the process of recovering pollutants must be fast, while also being efficient.

If the concentration of a NaOH solution is not high enough, desorption cannot be achieved with this washing solution, as described by Alvarez et al. in 2004 [21]. However, a very high concentration of NaOH can promote the retention of the OH groups on the active sites and delay the subsequent adsorption step [19]. This phenomenon can explain the reduction in the MCPA amount adsorbed on the Merck AC regenerated with a 1M NaOH solution, as presented in Figure 7.

3.6. Regeneration by Basic Aqueous Washing Followed by Thermal Treatment

Since in the third regeneration cycle the amount of MCPA desorb decreased drastically on all ACs, these were then submitted to a thermal regeneration process. After three adsorption–regeneration cycles, the ACs were separated from the washing solutions and regenerated by thermal treatment under nitrogen flux at 573 K for 30 min. The regenerated ACs were then used for a fourth cycle of MCPA adsorption, from the aqueous phase. The regenerated Merck AC was able to adsorb between 54.2% and 78.9% of the MCPA adsorbed in the first cycle. Yet, the amounts adsorbed were 1.63 to 2.65 times higher than the amounts adsorbed in the previous step (R3).

The regenerated Norit 1240 X_p and Norit 1240 X_g ACs were used on a fourth adsorption cycle. Surprisingly, in all trials, the amount of MCPA adsorbed was higher than the amount adsorbed during the first cycle. In Norit 1240 X_p and Norit 1240 X_g, stronger adsorption seems to take place, and desorption through the washing methods was more difficult to achieve. It should be emphasized that unlike thermal regeneration, regeneration by washing procedures with various washing solutions enables the recovery and reuse of the adsorptive. However, thermal treatment is quite effective for the regeneration of Norit 1240 X AC in powder or granular form. These results are consistent with the reduction in the acidic functional groups identified in the FTIR spectra, demonstrating that the ACs with high basic character present a better performance in the removal of pesticides from the aqueous phase [27].

4. Conclusions

The Merck and Norit ACs, mainly in powder form, present high adsorption capacities concerning the removal of MCPA from water. A longer contact time is required to achieve equilibrium with granular Norit AC. This work is focused on the results concerning different MCPA-saturated AC regenerating methods, namely using ethanol washing, basic aqueous washing, and a two-step combined treatment. The results obtained in different steps in the MCPA adsorption–desorption cycles show that the use of ethanol has a high potential for removing MCPA from microporous adsorbents. However, mainly on granular AC, the combined treatment of the washing solutions followed by a thermal treatment at 573 K was more efficient in recovering the surface properties of the spent AC than the individual basic aqueous washing treatments. It was also clear that Merck-saturated AC was easy to regenerate through basic washing solutions than the Norit 1204 X AC. In Norit 1240 X_p and Norit 1240 X_g, a stronger adsorption interaction seems to take place, and desorption through the washing methods was more difficult to achieve.

Thermal treatment, however, is quite successful in regenerating Norit 1240 X AC in granular or powder form. The thermal treatment enables MCPA that has been trapped in the microporous volume to desorb. When compared with virgin AC (Norit 1240 X_g), regenerate ACs, particularly Norit 1240 X_g–RT, present a higher maximum MCPA adsorption capacity, which can be attributed to a widening of the pore entrance. The adsorption–desorption cycles were carried out in controlled experimental conditions, using desorption cycles of 72 h and adsorption cycles of 24 h. Increasing the contact time may increase the amount of MCPA desorbed and adsorbed. However, in practice, a very long contact time is a major limitation to the application of the process. The data from the kinetic studies of the MCPA adsorption were well described by the pseudo-second-order model, and the Weber–Morris model allows us to state that on Norit 1240 X_g, the limiting factor to MCPA adsorption and kinetics was the pore diffusion.

At present, washing methods for adsorbent regeneration using different solvents are not used at an industrial level. However, the investigation of environmentally friendly regeneration methods is necessary to reduce energy consumption in thermal regeneration and achieve the objective of the circular economy.

Author Contributions: Conceptualization, I.P.d.P.C. and P.A.M.M.; methodology, J.E.d.S.F.C. and P.A.M.M.; validation, I.P.d.P.C. and P.A.M.M.; formal analysis, I.P.d.P.C. and P.A.M.M.; investigation, I.P.d.P.C. and P.A.M.M.; writing—original draft preparation, P.A.M.M. and I.P.d.P.C.; writing—review and editing, I.P.d.P.C., J.E.d.S.F.C. and P.A.M.M.; project administration, I.P.d.P.C., J.E.d.S.F.C. and P.A.M.M.; funding acquisition, I.P.d.P.C. and P.A.M.M.; All authors have read and agreed to the published version of the manuscript.

Funding: This work was funded by National Funds through FCT/MCTES—Portuguese Foundation for Science and Technology within the scope of the project UIDB/50006/2020. National Funds through FCT/MCTES from MED & CHANGE Research Centres within the scope of the project UIDB/05183/2020.

Informed Consent Statement: Not applicable.

Data Availability Statement: Not applicable.

Conflicts of Interest: The authors declare no conflict of interest.

References

1. He, H.; Liu, Y.; You, S.; Liu, J.; Xiao, H.; Tu, Z. A Review on Recent Treatment Technology for Herbicide Atrazine in Contaminated Environment. *Int. J. Environ. Res. Public Health* **2019**, *16*, 5129. [[CrossRef](#)] [[PubMed](#)]
2. Kulaishin, S.A.; Vedenyapina, M.D.; Kurmysheva, A.Y. Influence of the Surface Characteristics of Activated Carbon on the Adsorption of Herbicides (A Review). *Solid Fuel Chem.* **2022**, *56*, 181–198. [[CrossRef](#)]
3. Baskar, A.V.; Bolan, N.; Hoang, S.A.; Sooriyakumar, P.; Kumar, M.; Singh, L.; Jasemizad, T.; Padhye, L.P.; Singh, G.; Vinu, A.; et al. Recovery, regeneration and sustainable management of spent adsorbents from wastewater treatment streams: A review. *Sci. Total. Environ.* **2022**, *822*, 153555–153579. [[CrossRef](#)]

4. Sun, Y.; Zhang, B.; Zheng, T.; Wang, P. Regeneration of activated carbon saturated with chloramphenicol by microwave and ultraviolet irradiation. *Chem. Eng. J.* **2017**, *320*, 264–270. [[CrossRef](#)]
5. Zhang, L.-Q.; Jiang, H.-T.; Ma, C.-Y.; Yong, D. Microwave regeneration characteristics of activated carbon for flue gas desulfurization. *J. Fuel Chem. Technol.* **2012**, *40*, 1366–1371. [[CrossRef](#)]
6. González-Poggini, S.; Rosenkranz, A.; Colet-Lagrange, M. Two-Dimensional Nanomaterials for the Removal of Pharmaceuticals from Wastewater: A Critical Review. *Processes* **2021**, *9*, 2160. [[CrossRef](#)]
7. Cansado, I.P.d.P.; Belo, C.R.; Mourão, P.A.M. Valorisation of Tectona Grandis tree sawdust through the production of high activated carbon for environment applications. *Bioresour. Technol.* **2018**, *249*, 328–333. [[CrossRef](#)]
8. Cansado, I.P.d.P.; Mourão, P.A.M.; Belo, C.R. Using Tectona Grandis Biomass to Produce Valuable Adsorbents for Pesticide Removal from Liquid Effluent. *Materials* **2022**, *15*, 5842. [[CrossRef](#)]
9. Husien, S.; El-Taweel, R.M.; Salim, A.I.; Fahim, I.S.; Said, L.A.; Radwan, A.G. Review of activated carbon adsorbent material for textile dyes removal: Preparation, and modelling. *Curr. Res. Green Sustain. Chem.* **2022**, *5*, 100325–100340. [[CrossRef](#)]
10. Cazetta, A.L.; Junior, O.P.; Vargas, A.M.; da Silva, A.P.; Zou, X.; Asefa, T.; Almeida, V.C. Thermal regeneration study of high surface area activated carbon obtained from coconut shell: Characterization and application of response surface methodology. *J. Anal. Appl. Pyrolysis* **2013**, *101*, 53–60. [[CrossRef](#)]
11. Rao, M.M.; Ramana, D.; Seshaiyah, K.; Wang, M.; Chien, S.C. Removal of some metal ions by activated carbon prepared from Phaseolus aureus hulls. *J. Hazard. Mater.* **2009**, *166*, 1006–1013. [[CrossRef](#)] [[PubMed](#)]
12. Mourão, P.A.M.; Di Caprio, F.; Cansado, I.P.P.; Castanheiro, J.; Falcone, I.; Astolfi, M.L.; Pagnanelli, F. Granulation and activation of an arsenic adsorbent made of iron oxide doped hydrochar. *Chem. Eng. Trans.* **2022**, *93*, 91–96. [[CrossRef](#)]
13. Ouyang, J.; Zhou, L.; Liu, Z.; Heng, J.Y.; Chen, W. Biomass-derived activated carbons for the removal of pharmaceutical micropollutants from wastewater: A review. *Sep. Purif. Technol.* **2020**, *253*, 117536–117553. [[CrossRef](#)]
14. Ania, C.; Parra, J.; Menéndez, J.; Pis, J. Microwave-assisted regeneration of activated carbons loaded with pharmaceuticals. *Water Res.* **2007**, *41*, 3299–3306. [[CrossRef](#)] [[PubMed](#)]
15. Omorogie, M.O.; Babalola, J.O.; Unuabonah, E.I. Regeneration strategies for spent solid matrices used in adsorption of organic pollutants from surface water: A critical review. *Desalinat. Water Treat.* **2016**, *57*, 518–544. [[CrossRef](#)]
16. Nahm, S.W.; Shim, W.G.; Park, Y.-K.; Kim, S.C. Thermal and chemical regeneration of spent activated carbon and its adsorption property for toluene. *Chem. Eng. J.* **2012**, *210*, 500–509. [[CrossRef](#)]
17. Hwang, S.Y.; Lee, G.B.; Kim, J.H.; Hong, B.U.; Park, J.E. Pre-Treatment Methods for Regeneration of Spent Activated Carbon. *Molecules* **2020**, *25*, 4561. [[CrossRef](#)]
18. Román, S.; Ledesma, B.; González, J.; Al-Kassir, A.; Engo, G.; Álvarez-Murillo, A. Two stage thermal regeneration of exhausted activated carbons. Steam gasification of effluents. *J. Anal. Appl. Pyrolysis* **2013**, *103*, 201–206. [[CrossRef](#)]
19. Salvador, F.; Martín-Sánchez, N.; Sánchez-Hernández, R.; Sánchez-Montero, M.J.; Izquierdo, C. Regeneration of carbonaceous adsorbents. Part I: Thermal Regeneration. *Microporous Mesoporous Mater.* **2015**, *202*, 259–276. [[CrossRef](#)]
20. Salvador, F.; Martín-Sánchez, N.; Sánchez-Hernández, R.; Sánchez-Montero, M.J.; Izquierdo, C. Regeneration of carbonaceous adsorbents. Part II: Chemical, Microbiological and Vacuum Regeneration. *Microporous Mesoporous Mater.* **2015**, *202*, 277–296. [[CrossRef](#)]
21. Soto, M.L.; Moure, A.; Domínguez, H.; Parajó, J.C. Recovery, concentration and purification of phenolic compounds by adsorption: A review. *J. Food Eng.* **2011**, *105*, 1–27. [[CrossRef](#)]
22. Álvarez, P.; Beltrán, F.; Gómez-Serrano, V.; Jaramillo, J.; Rodríguez, E. Comparison between thermal and ozone regenerations of spent activated carbon exhausted with phenol. *Water Res.* **2004**, *38*, 2155–2165. [[CrossRef](#)] [[PubMed](#)]
23. Pak, S.-H.; Jeon, Y.-W. Effect of vacuum regeneration of activated carbon on volatile organic compound adsorption. *Environ. Eng. Res.* **2017**, *22*, 169–174. [[CrossRef](#)]
24. Larasati, A.; Fowler, G.D.; Graham, N.J. Extending granular activated carbon (GAC) bed life: A column study of in-situ chemical regeneration of pesticide loaded activated carbon for water treatment. *Chemosphere* **2022**, *286*, 131888–131998. [[CrossRef](#)] [[PubMed](#)]
25. Mourão, P.A.; Carrott, P.J.; Carrott, M.M.R.; Marques, L. Different Ways to Regenerate an Activated Carbon: Comparison between an Activated Carbon from Cork and a Commercial Carbon. *Mater. Sci. Forum* **2008**, *587–588*, 844–848. [[CrossRef](#)]
26. Liao, P.; Yuan, S.; Xie, W.; Zhang, W.; Tong, M.; Wang, K. Adsorption of nitrogen-heterocyclic compounds on bamboo charcoal: Kinetics, thermodynamics, and microwave regeneration. *J. Colloid Interface Sci.* **2013**, *390*, 189–195. [[CrossRef](#)] [[PubMed](#)]
27. Cansado, I.P.d.P.; Mourão, P.A.M.; Morais, I.D.; Peniche, V.; Janeirinho, J. Removal of 4-Ethylphenol and 4-Ethylguaiaicol, from Wine-like Model Solutions, by Commercial Modified Activated Carbons Produced from Coconut Shell. *Appl. Sci.* **2022**, *12*, 11754. [[CrossRef](#)]
28. Belo, C.R.; Cansado, I.P.d.P.; Mourão, P.A.M. Synthetic polymers blend used in the production of high activated carbon for pesticides removals from the liquid phase. *Environ. Technol.* **2017**, *38*, 285–296. [[CrossRef](#)]
29. Spaltro, A.; Pila, M.; Simonetti, S.; Álvarez-Torrellas, S.; Rodríguez, J.G.; Ruiz, D.; Compañy, A.D.; Juan, A.; Allegretti, P. Adsorption and removal of phenoxy acetic herbicides from water by using commercial activated carbons: Experimental and computational studies. *J. Contam. Hydrol.* **2018**, *218*, 84–93. [[CrossRef](#)] [[PubMed](#)]
30. Food and Agriculture Organization for the United Nation. FAO Specifications and Evaluations for Agricultural Pesticides. 2022. Available online: <https://www.fao.org/3/cc4226en/cc4226en.pdf> (accessed on 22 July 2023).

31. Simonin, J.P. On the comparison of pseudo-first order and pseudo-second order rate laws in the modeling of adsorption kinetics. *Chem. Eng. J.* **2016**, *300*, 254–263. [[CrossRef](#)]
32. Tochetto, G.A.; Brandler, D.; Pigatto, J.; Pasquali, G.D.L.; Alves, A.A.d.A.; Kempka, A.P.; da Luz, C.; Dervanoski, A. Kinetic modeling of the adsorption and desorption of metallic ions present in effluents using the biosorbent obtained from *Syagrus romanzoffiana*. *Environ. Monit. Assess.* **2023**, *195*, 844–902. [[CrossRef](#)] [[PubMed](#)]
33. Revellame, E.D.; Fortela, D.L.; Sharp, W.; Hernandez, R.; Zappi, M.E. Adsorption kinetic modeling using pseudo-first order and pseudo-second order rate laws: A review. *Clean. Eng. Technol.* **2020**, *1*, 100032–100045. [[CrossRef](#)]
34. An, F.-Q.; Wu, R.-Y.; Li, M.; Hu, T.-P.; Gao, J.-F.; Yuan, Z.-G. Adsorption of heavy metal ions by iminodiacetic acid functionalized D301 resin: Kinetics, isotherms and thermodynamics. *React. Funct. Polym.* **2017**, *118*, 42–50. [[CrossRef](#)]

Disclaimer/Publisher's Note: The statements, opinions and data contained in all publications are solely those of the individual author(s) and contributor(s) and not of MDPI and/or the editor(s). MDPI and/or the editor(s) disclaim responsibility for any injury to people or property resulting from any ideas, methods, instructions or products referred to in the content.